

# **Loss-of-Field Protection Relay Coordination for Synchronous Generator and Motor Unit Based on Transient Stability**

**Shengen Chen, Mohamad Musavi, Paul Villeneuve**

**University of Maine, Orono, ME**

**Paul Lerley**

**RLC Engineering, Hallowell, ME**

Presented to the

42<sup>nd</sup> Annual

Western Protective Relay Conference

Spokane, WA

October 20-22, 2015

**Abstract:** In order to maximize grid reliability, North American Electric Reliability Corporation (NERC) has requested that generator owners and transmission operators ensure proper coordination between plant equipment and transmission protection systems. The NERC criteria are meant to assure that generators remain on line to provide short term support during adverse grid conditions. A system stability study is required to evaluate generator and system response to power system faults and to subsequently evaluate if protective relays cause undesirable generator trips for recoverable events, particularly for the loss-of-field protection which may sometimes have default typical setting values or obsolete settings due to system growth. The typical relay settings may be acceptable in many instances. However; a recent review of loss-of-field relay settings for a synchronous machine operating as a generator and motor found that the same relay settings were used for both modes. This paper will address if these settings are appropriate.

## **1. Introduction**

Under NERC's power plant and transmission system protection coordination criteria [1], relay settings need to be ensured that machines are available for grid support during adverse conditions. A system stability study is required to evaluate a generator and system response to power system faults and to subsequently verify that the settings of its protective relays result in correct operation, especially for recoverable events. Since out-of-step (OOS) and loss-of-field (LOF) protective devices must trip only for non-recoverable events, their settings are very important to ensure stability. The concern was identified during the August 2003 blackout [2] that could have been prevented if proper relay settings were applied to specific generator relays. Reference [3] provides practical guidance for the coordination of specific protection areas such as generator capability curve, automatic voltage regulator, under excited and over-excited coordination, and V/Hz limiter with over-excitation (V/Hz). Usually, the generator protective relay settings are coordinated with the steady state stability limit and the generator capability curves. Performance of generator protection during major system disturbances is discussed in [4]. More protection relay functions [1] are described in detail. Many functions need the coordination between generator and transmission owners. The LOF protection function (40) and OOS protection function (78) must be coordinated via stability studies.

A novel method is presented to test the settings security of synchronous generator and motor LOF relays under selected system disturbances in this paper. First, the transient stability study considers various system conditions with variable loading of the unit, system dispatches, system loads and contingencies. The apparent impedance trajectories generated through the stability simulations are plotted over the relay R-X characteristic diagram. The two-dimensional superimposed R-X plots do not reveal the system swing time variable which determines the critical relay setting. The proposed methodology uses the relay characteristic mathematical model which allows an algorithm to compare the relay characteristic points to the apparent impedance trajectory simulation steps in the time domain. In other words, the time delay settings could be found by associating the R-X points to events in the time domain. Furthermore, the range of time delay settings is suggested by the model. If the relay trips incorrectly for the stable, recoverable swings or

does not trip correctly for legitimate LOF conditions, then the range of the offset is also recommended by the model.

This paper reviews general synchronous machine stability and general operating principles of typical LOF relays. The analysis of the impact of the generator and motor stability and system conditions is demonstrated. The proposed methodology was tested on a distance type LOF relay applied to a machine in a pumped storage generating site. Through a series of dynamic simulations the machine performance for the existing relay settings and for the suggested values derived from the proposed methodology are compared. The proposed methodology derives LOF protection parameter settings from systematic transient simulations, greatly enhancing confidence in the generators protection system and could be applied to OOS protection as well.

## 2. Generator and Motor Stability

### 2.1 A Simple System Equivalent

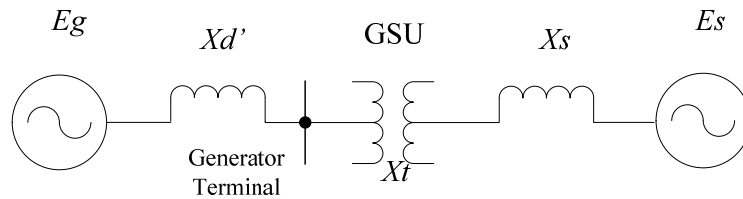


**Figure 1. Simplified equivalent system**

Synchronous generators operating in an interconnected power system all operate at synchronous speed under steady-state conditions. There is equilibrium between the total mechanical input to the turbines and the total electrical power output (plus losses) from the generators. This balance is maintained during normal load variations by the action of the turbine governors. Figure 1 shows a simplified synchronous machine and an equivalent system. This is a simplified model of the interconnected power system seen from a generator before adding any other factors into consideration for transient stability studies. The machine is based on ideal assumptions [6] in order to reduce the complexity of the stability analysis. The real power transfer curve can be expressed by:

$$P = \frac{E_g E_s}{X} \sin \delta \quad (1)$$

where  $X = X_d' + X_t + X_s$  is the total reactance between the two voltages,  $X_d'$  is the direct-axis transient reactance,  $X_s$  is an equivalent source impedance,  $X_t$  is the generator step up transformer (GSU) impedance, and  $\delta$  is the phase angle difference between the generator voltage  $E_g$  and the system voltage  $E_s$ .

## 2.2 Equal Area Criterion

Figure 2 shows the power and angle curves for the generator and motor. The discussion below is based on generator operation. However, the generator and motor share similar principles. The more realistic power-angle curve has damping included [7] and is much more complicated to convey the message. As a result, the ideal power-angle curve is selected for the following discussion.

The power transfer relationship at steady state can be described by the familiar power-angle curve (top line) shown in Figure 2. Starting from power transfer  $P = 0$  and as it increases,  $\delta$  follows the increasing trend until it reaches 90 degrees, and the real power has its maximum value at  $P_{MAX}$ . After this point, the further increase of  $\delta$  will result in a decrease of power transfer. Neglecting losses,  $P_0$  equals the mechanical power  $P_M$  delivered from the turbine shaft, which is constant. The synchronous generator is operating at an equilibrium point with the interconnected power system and balance is maintained. At the pre-fault equilibrium point A, the rotor runs at a constant speed.

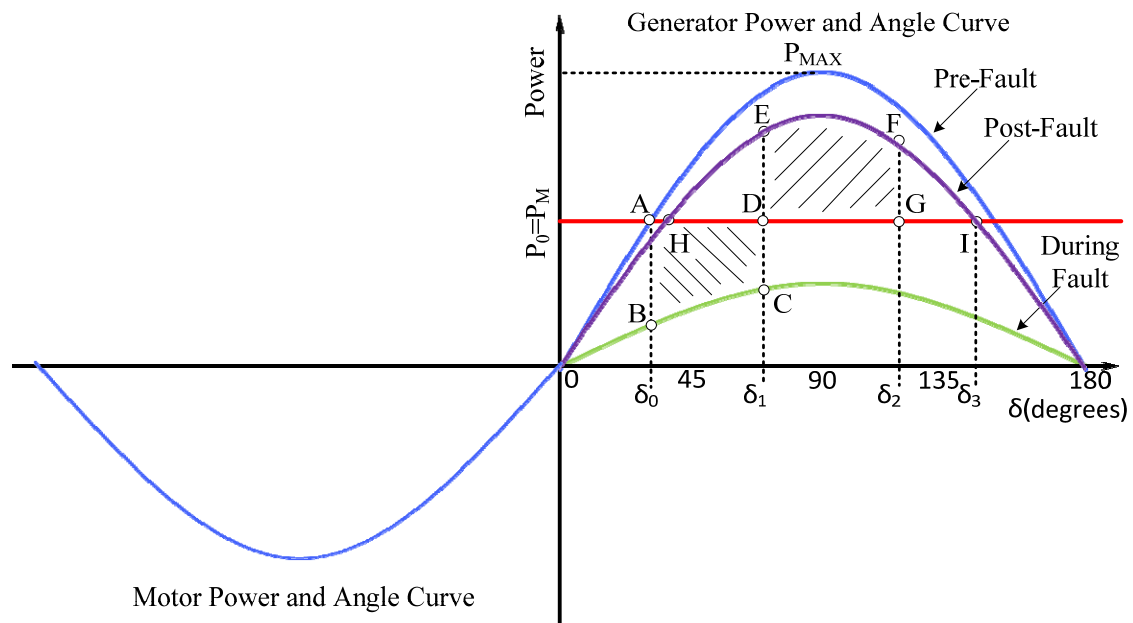


**Figure 2. Power and angle curve for generator and motor, and equal area criterion**

During normal operating conditions, the generator is able to transfer real power according to the relationship of the power-angle curve described previously along with a Thévenin equivalent impedance. When a fault occurs, the impedance varies and the power-angle curve changes from the pre-fault curve to during fault curve as shown in right side of Figure 2. When the fault occurs the rotor angle is at the pre-fault value  $\delta_0$ . Since the prime mover input power now exceeds the electrical output, the generator accelerates until the fault is cleared, at which time the angle has reached  $\delta_1$ . At this point the rotor starts decelerating because the electric power at  $\delta_1$  is now larger than the mechanical power  $P_0$  (assumed to remain constant). Thus the accelerating energy is shaded as the area ABCD and the decelerating energy is shaded as the area DEFG (shown in Figure 2). If the area DEFG is bigger than ABCD, the generator goes to a new balance point H after sufficient

damping. The new equilibrium point occurs if the post-fault system topology was changed by the protective relays action, which alters the post fault impedance seen by the generator. The equal area criterion states that the generator remains stable only if the decelerating energy is larger or at least equal to the accelerating energy. This can only occur while the electrical output power (load) exceeds the mechanical input power. Point I in Figure 2 marks the boundary of this condition. When the decelerating area extends to point I and is equal to the accelerating energy area, the rotor angle  $\delta_1$  defines the critical clearing angle. If the area EDI is less than the area ABCD, the rotor will continue to advance, the electrical power transfer will continue to decrease and the rotor will not recover to a stable equilibrium position. This situation represents transient instability where the generator is out of step (OOS) with the system.

### 2.3 Apparent Impedance

Each generator can be considered as a node connected to the rest of the power system through the apparent impedance. shows the connection between a generator bus and the rest of the system.

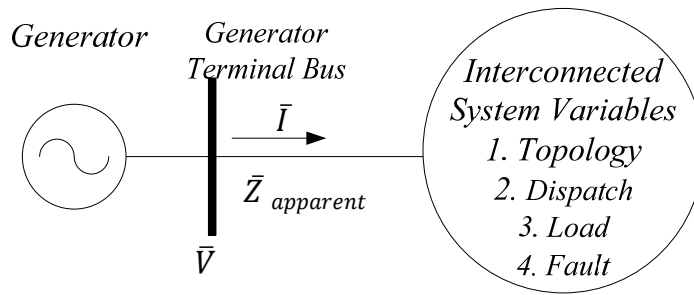


**Figure 3. The apparent impedance between a generator and the rest of the system**

The main attributes of the generators considered in this investigation are inertia, real power, reactive power and initial rotor angle. The pertinent system states are its topology, dispatch, load, and the potential for faults occurring at different locations with various durations and types. Thus the initial apparent impedance is defined by the initial states of the generator and the system at steady state. When a fault occurs on the power grid, the apparent impedance seen at the generator node is instantly changed by an amount depending on the electric distance between the generator and the fault. The generator output current experiences a corresponding increase which results in voltage sag at the generator terminal due to voltage drop across the generator internal impedance. These current and voltage changes define the instantaneous apparent impedance seen by the generator. The trajectory of the apparent impedance also represents the fluctuation of real and reactive power flow between the generator and system. The following equations describe these relationships [8]:

$$\bar{Z}_{app} = \frac{\bar{V}}{\bar{I}} = R + jX \quad (2)$$

where

$$R = \frac{V^2 P}{P^2 + Q^2} = vP \quad (3)$$

$$X = \frac{V^2 Q}{P^2 + Q^2} = vQ \quad (4)$$

By dividing (3) and (4), the R/X and P/Q ratio relationship is obtained:

$$\frac{R}{X} = \frac{vP}{vQ} = \frac{P}{Q} \quad (5)$$

Also note that  $v$  is based on the squared voltage magnitude to the apparent base power. While (5) shows the equal ratios, this means the close relationship between R-X and P-Q diagram. However, it does not mean the R and P have a fixed ratio,  $v$  varies due to the square of voltage magnitude when a disturbance occurs.

### 3. Loss-of-Field Relay Principles

The offset mho relay has been widely adapted to provide LOF protection for modern synchronous generators [9], [10]. According to [11], a loss of supply to the excitation may cause serious operating conditions for both the generator and system. When the generator loses its excitation, it overspeeds and operates as an induction generator. Under LOF conditions the rotor temperature increases rapidly, overloading the stator winding due to the eddy currents caused by slip. Consequentially, a serious overheating risk might occur. Synchronous generators are not designed to operate as induction machines.

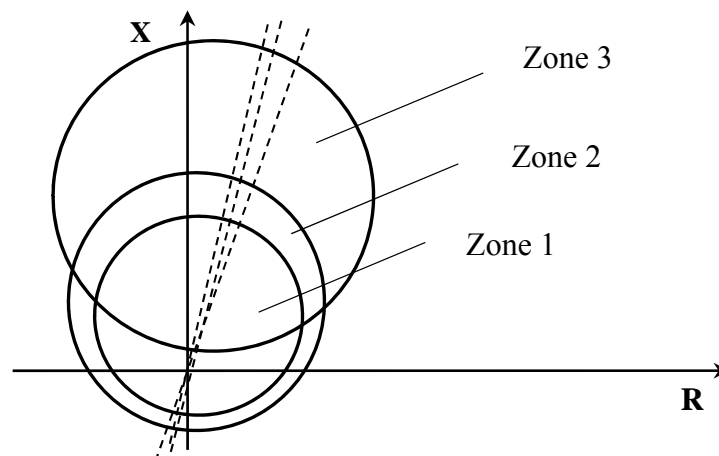


**Figure 4. Mho distant relay**

While loss of field is an extreme form of excitation failure, operating a generator with reduce field weakens magnetic coupling between the rotor and stator, which could result in loss of synchronism if the mechanical and electrical power are not in balance. The generator would then be in an out of step (OOS) mode, a condition similar to the loss of field where the eddy currents would rapidly overheat the rotor steel. Therefore, the closely related LOF and OOS must be considered in the study of relay coordination.

## **4. Loss-of-Field Coordination Process and Methodologies**

### **4.1 Relay Coordination Process**

Figure 5 describes the LOF relay coordination process. The transient stability simulation converts the existing relay settings to generate apparent impedance data. Consequently, the data are passed through the setting assessment for the relay setting verification.

Typically, planning and operation engineers conduct transient stability studies with the impedances expressed in per-unit of the system base impedance, usually on a 100 MVA base, while relay engineers work in either primary or secondary (relay) ohms. This means that data format conversion from one to another is required [3]. In this paper the apparent impedance trajectory is expressed in per-unit of the system base impedance [12].

After the conversion calculation of the existing relay settings given by the generator and transmission entities, the relay characteristic for the existing relay settings is ready for the transient stability simulation and assessment process usage. For a systematic assessment of the system stability performance, testing a large number of faults against a considerable number of system conditions is recommended and can be performed with automated batch simulations. It is reasonable to draw from historical results to select the most significant or the worst scenarios.

The transient stability simulation has to consider different combination scenarios such as dispatch, fault type and fault clearing time for a given network topology. The apparent impedance data generated from the transient stability simulation is superimposed with the relay characteristic. If the existing relay settings result in relay trip commands for all non-recoverable events, they are considered reliable and secure. Then, the existing settings are well coordinated with the interconnected system and the assessment process is finished. Otherwise, new recommended settings must be tested again to check if any other violations are present. The lower limit and upper limit of the new relay settings and time delay settings are defined for a secure and reliable condition where no violation is found.

Note that this process is validated for both LOF and OOS relay coordination. The case study in next section will describe the details of the process for LOF relay coordination. The case study examined pump storage units that only have LOF relay. However, if the OOS relay presents, then it is suggested to have the proposed coordination review process.

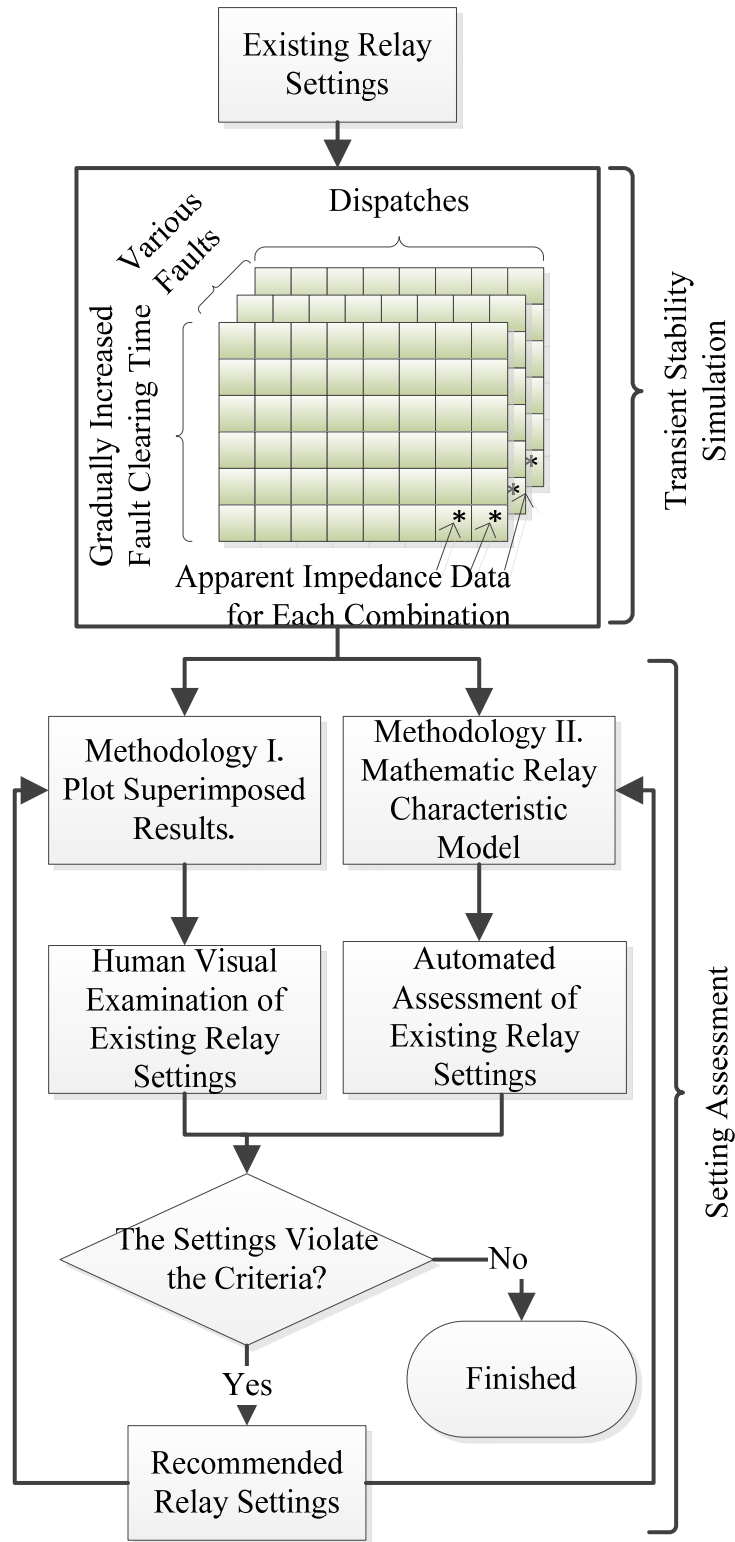


**Figure 5. Relay coordination process.**



## 4.2 Superimposed Plot and Human Visual Assessment

The superimposed plot approach, as shown on the left-hand side blocks of Figure 5, uses the apparent impedance trajectory and relay characteristic plot in R-X diagram. The conventional method only checks the superimposed plot of the whole apparent impedance trajectory and relay characteristic. The two-dimensional R-X is not sufficient to verify that the LOF relay will trip or block tripping when subjected to a system swing. The relay trip time delay, necessary to differentiate between line faults and system swings (the apparent impedance changes are slower during the post fault swings) must also be known. In the manual analysis process short groups of the apparent impedance data of a specific time duration chosen by the planner, are gradually plotted over the relay characteristic (simulating an animation). The Planner then looks for and records the times when the apparent impedance crosses the relay characteristic boundaries to determine the duration that the impedance locus stayed inside the trip zone. Although, the three dimensions of the R-X diagram with time would also be a solution for time delay setting, the examination for three-dimension plot is more difficult since the complexity is increased. Due to the large number of plots, which are multiplied by the gradually increased time and combination of system conditions, the examination of superimposed plots could be time consuming, tedious and result in lack of accuracy.

## 4.3 Mathematical Model and Automated Assessment

In this approach, the automated assessment extracts the apparent impedance data and passes it to the mathematical model to assess the relay coordination. The advantage of this methodology is in associating the relay characteristics to events in the time domain. This is demonstrated in Figure 6, which shows the boundaries of the LOF relay characteristics. The regions of the boundary conditions 1, 2 and 3 as shown in Figure 6 are defined in Table 1.

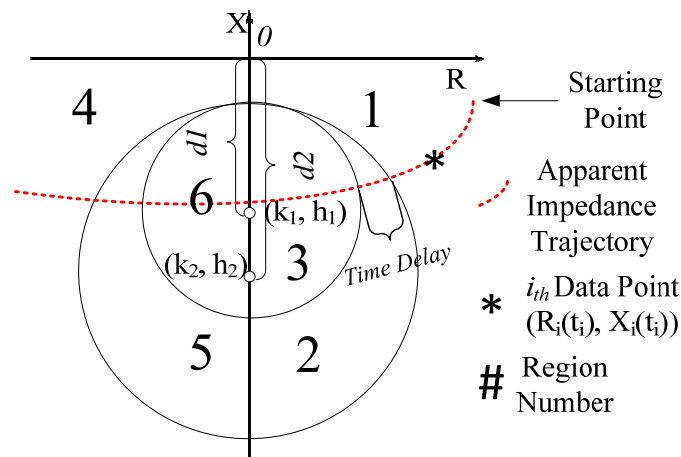


**Figure 6. A double circle loss-of-field relay characteristics**

The time interval between the consequent apparent impedances, i.e.  $i$ th and  $(i-1)$ th, on the trajectory is a quarter cycle (4 milliseconds) time step, which is the simulation time resolution commonly used by modern simulation software. Note that  $R_i$  is the apparent

resistance and  $X_i$  is the apparent reactance at time  $t_i$ . In general, the relay characteristic is a combination of circles or lines which could be expressed in boundary functions. The boundaries define the close or open spaces as regions that are used to track the apparent impedance position during the swing.

| Region Number | Boundary Conditions   |
|---------------|---|
| 1             | Outside of Zone 2 Characteristic & Positive R                                   |
| 2             | Inside of Zone 2 Characteristic & Outside of Zone 1 Characteristic & Positive R |
| 3             | Inside of Zone 1 Characteristic & Positive R                                    |
| 4             | Outside of Zone 2 Characteristic & Negative R                                   |
| 5             | Inside of Zone 2 Characteristic & Outside of Zone 1 Characteristic & Negative R |
| 6             | Inside of Zone 1 Characteristic & Negative R                                    |

**Table 1. Region boundary conditions for LOF relay**

The activity of the tripping command of relay is defined by the regions of Table I in R-X plane. The following information (per unit on 100MVA base) is given by the LOF relay (Figure 6):

- Zone 1 offset in direction of generator =  $d1 \angle \theta 1^\circ$
- Zone 2 offset in direction of generator =  $d2 \angle \theta 2^\circ$
- Zone 1 mho circle diameter =  $D1$ , radius  $r1 = D1/2$
- Zone 2 mho circle diameter =  $D2$ , radius  $r2 = D2/2$
- Zone 1 mho circle center( $k1, h1$ )
- Zone 2 mho circle center( $k2, h2$ )

Two basic boundary functions that normally determine the six boundary regions are:

$$(U - k_1)^2 + (V - h_1)^2 = r_1^2 \quad (6)$$

$$(U - k_2)^2 + (V - h_2)^2 = r_2^2 \quad (7)$$

$U$  is the apparent resistance variable (R) and  $V$  is the apparent reactance (X). Equations (6) and (7) define the zone 1 and 2 mho circle, which three regions 1, 2, and 3, as shown in Figure 6 and Table 1. The LOF relay model shares the same principles in defining the boundary conditions as in the OOS relay model. In fact, this methodology is applicable to any type of mho relay. The time delays shown in Figure 6 can be calculated by the subtraction of the time of the impedance trajectory crossing between the mho circles (LOF relay). See the detailed examples in the following case study.

At any time during a contingency, the location of the instantaneous apparent impedance ( $R_i(t_i), X_i(t_i)$ ) could be located on the regions of Figure 6 that are determined by equations (6) and (7). The following processes give an example of how to define the boundary conditions.

1. Substitute data  $X_i(t_i)$  and  $(R_i(t_i))$  into equation (6) and (7).
2. To determine if data is in which region, outside or inside of the circle, it is necessary to calculate the value of  $(X_i(t_i)-k_1)^2 + (R_i(t_i)-h_1)^2$  and  $(X_i(t_i)-k_2)^2 + (R_i(t_i)-h_2)^2$ .
3. If  $r_1$  is bigger than  $(X_i(t_i)-k_1)^2 + (R_i(t_i)-h_1)^2$ , the apparent impedance is outside of zone 1 circle.
4. If  $r_2$  is bigger than  $(X_i(t_i)-k_2)^2 + (R_i(t_i)-h_2)^2$ , the apparent impedance is outside of zone 2 circle.
5. Also determine if data on right or left side of vertical axis with positive or negative R.

#### **4.4 Relay Settings Coordination Criteria Decision**

The determination of the travel times of the apparent impedance on its trajectory through the manual superimposed plot methodology is tedious and time consuming. However, this obstacle can be overcome with the mathematical model and its automated assessment methodology. The mathematical model compares the relay characteristic to the apparent impedance trajectory simulation steps in the time domain. In other words, the time delay settings are found by associating the R-X trajectory to events in the time domain. The criteria used in relay coordination process, shown in Figure 5, include factors such as the generator stability, the region that apparent impedance trajectory passes through, and the time settings.

The time series of regions represent the relationship of the relay characteristic and the apparent impedance trajectory in time domain. Therefore, the apparent impedance trajectory can be transformed to a time series of regions with the time traveling in each region. From this information, it can be determined if the relay operation is secure and reliable based on appropriate transient stability simulations.

#### **4.5 Recommendation for Settings Adjustment**

There are two improper relay settings that could be adjusted by using the proposed mathematical model described above. These are when the existing relay settings are found to: 1) trip for stable/recoverable swings and 2) not trip for legitimate LOF conditions. In both cases, the range of the relay characteristic reach, offsets and time settings of the proposed mathematical model could be used to adjust the improper relay settings. To do this a new adjustment variable ( $\eta$ ) could be used to define the required offsets  $d_1+\eta$  and  $d_2+\eta$  for LOF relay. The adjustment variable  $\eta$  has a lower and upper range ( $\eta_L, \eta_U$ ) that satisfies the condition for correcting the improper relay settings. Therefore, a range of time settings could also be suggested by corresponding to the range of the offsets.

### **5. Case Studies**

The case study is intended to compare the result of the proposed methodology with the existing generator and motor protective device settings for LOF (function 40) conditions. The study was conducted based on NERC's protection coordination guidance [1]. A

pump storage unit connected to a 345kV bus in the Eastern North American Power System (ENPAS) is used to show the proposed relay coordination methodology. Both modes have used the same existing LOF settings. The proposed methodology was used to show the effectiveness of examining if improper relay settings exist.

## 5.1 Faults

Two most significant contingencies (faults) are applied to examine the transient performance of system and to test the generator in this paper. Figure 7 shows the location of these two faults: a three phase fault on the utility 345 kV bus and a SLG fault on Line 1 with breaker 1T failure. A short circuit model is used to obtain negative-sequence and zero-sequence impedances for the SLG fault impedance representation in the single line system model. These contingencies were chosen since the faults near the study unit cause faster swings and are therefore more difficult to differentiate from line faults. The station would require shorter clearing times, and the timing setting is therefore more critical and relay is more likely to be insecure.

For each fault, the clearing time was increased incrementally until the generator became unstable. When the last stable increment was found, the resolution was changed to be equal or less than half a cycle to achieve a higher resolution. Thus, the critical clearing time could be determined by the sequential fault clearing time applied. The cases were then analyzed by stability criteria. For each fault, twelve dispatches were considered. The impedance locus for the twelve dispatches were checked against the relay characteristic to determine if the relays would trip for this recoverable case. Obviously, no tripping should occur for this condition. The impedance locus for the unstable case should be also checked to assure that the impedance locus passes through the tripping characteristic.

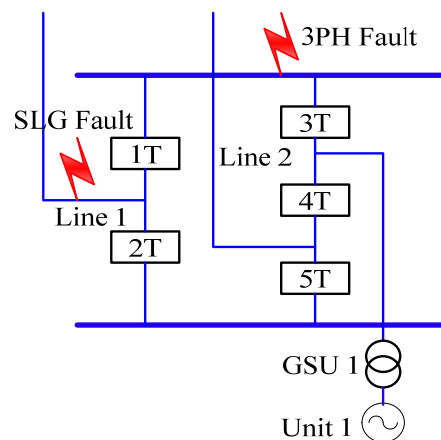


**Figure 7. One line diagram at pump storage generating site**

## 5.2 Dispatch

Six dispatches (D1a\_G, D1\_G, D2a\_G, D2\_G, D3a\_G, D3b\_G) with the unit in generator mode and six dispatches (D1a\_P, D1\_P, D2a\_P, D2\_P, D3a\_P, D3b\_P) with the unit in pump mode were used to test a range of system conditions, including

variations in the selected interface flow and variations in the real and reactive power output of the unit. Two different power flow levels (2000MW and 1000MW) are considered at an interface near the study region with three combinations of maximum or minimum values of real and reactive powers, as presented in Table 2. The combination of extreme real and reactive power loadings were used to test the generator and motor performance and coordination.

| Power Flow                    | 2000                          | 1000                          | 2000                          | 1000                          | 2000                          | 2000                          |
|-------------------------------|-------------------------------|-------------------------------|-------------------------------|-------------------------------|-------------------------------|-------------------------------|
| <b>Dispatch for Generator</b> | <b>D 1a_G</b>                 | <b>D 1_G</b>                  | <b>D 2a_G</b>                 | <b>D 2_G</b>                  | <b>D 3a_G</b>                 | <b>D 3b_G</b>                 |
| <b>Unit in Generator mode</b> | Max MW & Min MVA <sub>r</sub> | Max MW & Min MVA <sub>r</sub> | Min MW & Max MVA <sub>r</sub> | Min MW & Max MVA <sub>r</sub> | Max MW & Min MVA <sub>r</sub> | Max MW & Max MVA <sub>r</sub> |
| <b>Dispatch for Pump mode</b> | <b>D 1a_P</b>                 | <b>D 1_P</b>                  | <b>D 2a_P</b>                 | <b>D 2_P</b>                  | <b>D 3a_P</b>                 | <b>D 3b_P</b>                 |
| <b>Unit in Pump mode</b>      | Max MW & Min MVA <sub>r</sub> | Max MW & Min MVA <sub>r</sub> | Min MW & Max MVA <sub>r</sub> | Min MW & Max MVA <sub>r</sub> | Max MW & Min MVA <sub>r</sub> | Max MW & Max MVA <sub>r</sub> |

**Table 2. Dispatch summary**

### 5.3 Simulation

Transient simulations and plots are performed based on cluster computing technology [13]. Thirty seconds of transient simulation is tested with a 0.1 second pre-fault period before the application of the system disturbance with PSS/E. The given generator control models including exciter, governor, and power system stabilizer are active. In the case of system's abnormal performance, like a small signal disturbance, the control model is tuned up [14] and [15]. The quarter cycle simulation steps limit the time calculations to +/- 4 milliseconds accuracy. In this case study, twenty five 3 phase faults and thirty five of single line to ground faults described in section 5.1 were applied for each dispatch. Thus total  $(25+35)*6 + (25+35)*6 = 720$  simulations were run for both LOF relay coordination.

### 5.4 LOF Relay Coordination Results

#### 5.4.1 Existing Relay Coordination

Unit 1 of the case study, Figure 7, utilizes a same LOF relay with one zone and a single timing relay with an existing timer setting at 0.5 seconds for both generator and motor modes. The origin of the devices providing this protective function is located at the terminal of the generator.

The apparent impedance trajectories of fastest fault clearing time among all the generator mode dispatch and LOF relay characteristic were shown in Figure 8. The apparent impedance trajectories of fastest fault clearing time among all the pump mode dispatch and LOF relay characteristic were shown in Figure 9. Stable and unstable apparent impedance trajectories were applied with a three phase fault on the bus with 8 and 8.5 cycles fault clearing time, respectively, and are shown in Figure 8. Stable and unstable

apparent impedance trajectories were applied with the same three phase fault on the bus with 7.5 and 8 cycles fault clearing time, respectively, and are shown in Figure 9.

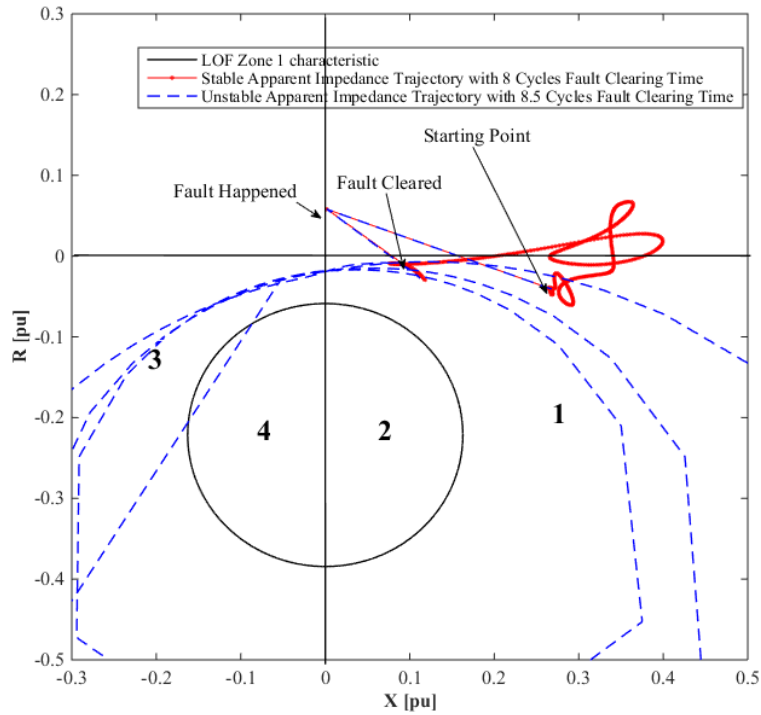


**Figure 8. LOF relay characteristic and the impedance trajectories of stable and unstable swings in the R-X plane under generator mode.**

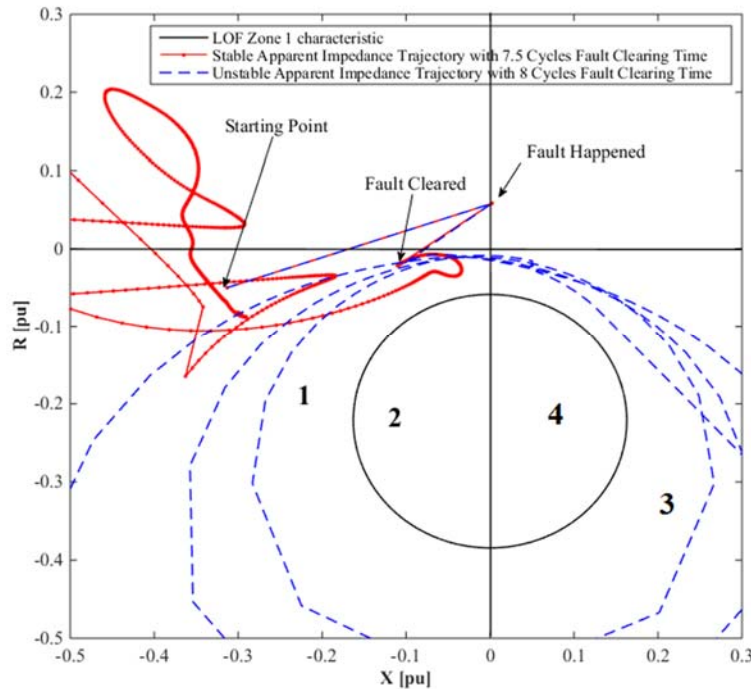


**Figure 9. LOF relay characteristic and the impedance trajectories of stable and unstable swings in the R-X plane under pump mode.**

### 5.4.2 Methodology I. Superimposed Plots

The apparent impedance trajectory plots (Figure 8 and 9) were added to the LOF relay characteristics to perform the relay coordination. Figure 8 shows two LOF superimposed plots of a stable and an unstable apparent impedance trajectories for generator mode. Each simulation applies superimposed plot methods to generate 77 plots for the trajectory animation in the time domain as described in section 4.2. Thus a total of  $360 \times 77 = 27720$  LOF superimposed plots are reviewed with the LOF relay coordination criteria for all the faults and dispatches for generator mode only. The review checked whether improper relay settings exist in the superimposed plots. Similarly, the review for pump mode was conducted.

According to the current setting, if during a power swing, the apparent impedance locus measured at the generator terminal passes into the LOF impedance characteristic circle zone 1, a timer is started. If the trajectory remains within region 2 long enough to allow the timer to timeout, the relay will issue a trip command.

The review of the superimposed plots of the LOF shows the relay protection coordinates with the rest of system. Unit 1 did not demonstrate instances where recoverable swings had an impedance locus pass into the tripping characteristic. The unrecoverable swings pass into zone 1, however, the times that apparent impedance trajectories pass into zone 1 and remain in region 2 are always very difficult to determine.

### 5.4.3 Methodology II. Mathematical Relay Model

| Time (sec) | Simulation Boundary Conditions (Regions) |  |
|------------|--|--|
|            | stable swing at 8 cycles                 | unstable swing at 8.5 cycles (existing ) |
| -0.0083    | 1  | 1  |
| ...        | 1  | 1 (repeat sequence)                      |
| ...        | 1  | 3 (repeat sequence)                      |
| 1.7459     | 1  | 3 (Tripped with infinite R & X value)    |
| 30.0028    | 1  | 3  |

**Table 3. LOF relay time series of boundary conditions for pump mode**

The mathematical LOF relay model utilizing the relay settings has been described in section 4.3. The mathematical relay model checks if any apparent impedance trajectories of 720 simulations violate the settings in time domain. The result shows that for all stable, recoverable swings the trip command does not issue, and all unstable swing, unrecoverable swings lead to issuing the trip command in all simulations. And most importantly, the model reveals that the trajectories do not pass into mho circle or do pass into the mho circle but remain inside less than the time delay setting 0.5 second.

For example, Table 3 shows the detailed data apparent impedance trajectories in Figure 8 were simulated by three phase fault at the substation bus with 8 and 8.5 cycles fault clearing time under the dispatch D3a\_G. The data were compared with LOF mathematical model, the time traveling in a region could be derived from this comparison. Each time traveling in zone 1 is less than the timer setting 0.5 second, thus

the result shows that the time delay setting 0.5 second is very secure. The stable swing is all in region 1, and an unstable swing has the repeated passage 1, 3 regions, which coordinate with the existing relay settings. Note that repeated passage 1, 3 regions mean the out of step status of the generator, after few cycles of out of step trajectory, the generator was tripped. Therefore, the relay could issue trip command when the unstable swing occurs, and the LOF coordination exists.

#### **5.4.4 LOF Recommendation Coordination**

As the all the trajectories have been passed through the setting assessment process, and no setting criteria violations were found, this case study is properly coordinated. As a result, the existing relay settings for the unit provides adequate margin for even the most severe recoverable power swings.

## **6. Conclusion**

This paper discusses transient stability, apparent impedance, and LOF protective function principles. The NERC stability criteria are applied into LOF coordination review, and the coordination process and relay setting assessment are demonstrated. The conventional superimposed plot method and proposed mathematical relay models with automated assessment are implemented for LOF relay coordination review. Following with the case study, the results are illustrated and interpreted. The use of the mathematical model enhances the efficiency and accuracy for the coordination of relay characteristics, especially, the relay time delay settings and relay setting adjustments. To avoid inappropriate relay operation for LOF conditions on pump storages, the protection scheme designs have to cooperate with transient stability study.

## **7. Reference**

- [1] North American Electric Reliability Corporation, "Power Plant and Transmission System Protection Coordination," July 2010.
- [2] U.S.-Canada Power System Outage Task Force, "Final Report on the August 14, 2003 Blackout in the United States and Canada: Causes and Recommendations," April, 2004.
- [3] Working Group J-5 of the Rotating Machinery Subcommittee, Power System Relay Committee, "Coordination of Generator Protection with Generator Excitation Control and Generator Capability," in *IEEE Power Engineering Society General Meeting*, 2007.
- [4] Working Group J6 of the Rotating Machinery Protection Subcommittee, Power System Relaying Committee, "Performance of Generator Protection During Major System Disturbances," *IEEE Transactions on Power Delivery*, vol. 19, no. 4, pp. 1650-1662, 2004.
- [5] New York Independent System Operator, "Transmission and Dispatching Operations Manual," New York Independent System Operator, Rensselaer, NY, December 2014.



- [6] J. D. Glover, M. S. Sarma and T. J. Overbye, "Transient Stability," in *Power System Analysis & Design*, January 3, 2011.
- [7] E. W. Kimbark, "Damper Winding and Damping," in *Power System Stability Volume III Synchronous Machines*, New York, John Wiley & Sons, Inc., 1956, pp. 243-244.
- [8] P. Kundur, *Power System Stability and Control*, Palo Alto, California: Electric Power Research Institute, 1993.
- [9] C. R. Mason, "A New Loss of Excitation Relay for Synchronous Generators," *AIEE Trans*, vol. 66, pp. 1240-1245, 1949.
- [10] J. Berday, "Loss of Excitation Protection for Modern Synchronous Generators," *IEEE Transactions on Power Apparatus and Synchronous Generators*, Vols. PAS-94, no. 5, pp. 1457-1463, 1975.
- [11] I. C37.102-2006, "Guide for AC Generator Protection, Section 4.5.1".
- [12] Siemens Power Technologies International, "PSSE32.0.5 Volume II Program Application Guide," in *Chapter 19 Transmission Line and Other Relay Models*, Schenectady, NY, Siemens Industry, Inc., October 2010.
- [13] K. Meng, Z. Dong and P. W. Kit, "Enhancing the Computing Efficiency of Power System Dynamic Analysis with PSS\_E," in *IEEE International Conference on Systems, Man, and Cybernetics*, San Antonio, TX, USA, October 2009.
- [14] M. J. Basler and R. C. Schaefer, "Understanding Power-System Stability," *IEEE Transactions on Industry Applications*, vol. 44, no. 2, pp. 463-474, 2008.
- [15] G. J. Dudgeon, W. E. Leithead, A. Dysko, J. O'Reilly and J. McDonald, "The Effective Role of AVR and PSS in Power Systems: Frequency Response Analysis," *IEEE Transactions on Power Systems*, vol. 22, no. 4, pp. 1986-1994, 2007.

**Shengen Chen** is Research Assistant for Maine Smart Grid & Intelligent Systems Laboratory at University of Maine. He received M.S. in electrical engineering from the University of Maine, Orono, ME, USA in 2013. Currently he is pursuing the Ph.D. degree at the Department of Electrical and Computer Engineering (with a minor in mathematics). His research areas include power system stability assessment, power system relay protection coordination and application of Synchrophasor in the smart grid. He is a student member of IEEE and CIGRE, and CIGRE study committee member for JWG D2/C2.41 and C6/D2.32.

**Mohamad Musavi** is Associated Dean of the College of Engineering and Professor of Electrical and Computer Engineering at University of Maine, USA. He received the M.S. and Ph.D. degrees in electrical engineering from the University of Michigan, Ann Arbor, MI, USA, in 1979 and 1983, respectively. He is currently the Associate Dean of the College of Engineering and a Professor of electrical and computer engineering at the University of Maine, Orono, ME, USA. His research interest is in the development of neural networks in a number of areas including power systems, smart grid, paper industry, genomics, and other applications.

**Paul Villeneuve** joined the Electrical Engineering Technology teaching team in 2003. He received the B.S. degree from Electrical Engineering Technology, University of Maine, 1993 and M.S. degree in Electrical Engineering, University of Maine, 1996. Paul teaches courses in electronics and control systems. He has spent the majority of his time as a consultant working on various tasks from submarine propulsion systems

to nuclear plant control systems. Paul is a registered professional engineer in the states of New York, Virginia, and New Hampshire. He consults on various projects to keep his knowledge current.

**Paul Lerley** is Senior Power System Engineer at RLC-Engineering, Hallowell, Maine. He received the BTS degree from the Lycée Technique, Strasbourg, France, in 1968 and the BET degree from the University of New Hampshire, Durham, NH, USA, in 1979. His professional journey included test engineering, power system protection applications, testing and training and currently power system simulations. He served on the PSRC.